Structural analysis of the catalytic mechanism and stereo selectivity in Streptomyces coelicolor alditol oxidase

Forneris, Federico; Heuts, Dominic P. H. M.; Delvecchio, Manuela; Rovida, Stefano; Fraaije, Marco W.; Mattevi, Andrea

Published in:
Biochemistry

DOI:
10.1021/bi701886t

Publication date:
2008

Structural Analysis of the Catalytic Mechanism and Stereoselectivity in *Streptomyces coelicolor* Alditol Oxidase[†,‡]

Federico Forneris,[||] Dominic P. H. M. Heuts,[§] Manuela Delvecchio,[||] Stefano Rovida,[||] Marco W. Fraaije,*[,§] and Andrea Mattevi*[,||]

Department of Genetics and Microbiology, University of Pavia, Via Ferrata 1, 27100 Pavia, Italy, and Laboratory of Biochemistry, Groningen Biomolecular Sciences and Biotechnology Institute, University of Groningen, Nijenborgh 4, 9747 AG, The Netherlands

Received September 14, 2007; Revised Manuscript Received November 6, 2007

ABSTRACT: Alditol oxidase (AldO) from *Streptomyces coelicolor* A3(2) is a soluble monomeric flavin-dependent oxidase that performs selective oxidation of the terminal primary hydroxyl group of several alditols. Here, we report the crystal structure of the recombinant enzyme in its native state and in complex with both six-carbon (mannitol and sorbitol) and five-carbon substrates (xylitol). AldO shares the same folding topology of the members of the vanillyl-alcohol oxidase family of flavoenzymes and exhibits a covalently linked FAD which is located at the bottom of a funnel-shaped pocket that forms the active site. The high resolution of the three-dimensional structures highlights a well-defined hydrogen-bonding network that tightly constrains the substrate in the productive conformation for catalysis. Substrate binding occurs through a lock-and-key mechanism and does not induce conformational changes with respect to the ligand-free protein. A network of charged residues is proposed to favor catalysis through stabilization of the deprotonated form of the substrate. A His side chain acts as back door that "pushes" the substrate-reactive carbon atom toward the N5−C4a locus of the flavin. Analysis of the three-dimensional structure reveals possible pathways for diffusion of molecular oxygen and a small cavity on the *re* side of the flavin that may host oxygen during FAD reoxidation. These features combined with the tight shape of the catalytic site provide insights into the mechanism of AldO-mediated regioselective oxidation reactions and its substrate specificity.

Carbohydrate oxidases are industrially interesting enzymes because of their ability to catalyze the oxidation of mono-, oligo-, and polysaccharides. These enzymes combine the capability to use the cheap and clean oxidant O_2 with high specificity and regioselectivity toward cheap and versatile carbohydrate substrates (*1*). Oxidation of sugars and their derivatives results in changed chemical and physical properties such as altered reductive power, solubility, gel strength, swelling, and chelation characteristics. Oxidized carbohydrates are applied, for example, as thickeners or emulsifiers in the food industry, as water binders in the paper industry, as metal chelators, or as antioxidizing agents in organ preservation (*2*). These compounds are also used as building blocks in chemical synthesis routes, as precursors for further chemical modification or for conjugation to other biomolecules (*3*). Most carbohydrate oxidases have been isolated from fungi, are predominantly active on mono- and/or disaccharides, and belong to a specific group of flavoproteins: the vanillyl-alcohol oxidase (VAO)[1] family (*1*). Members of this family share a similar overall structure consisting of two domains (*4*). One domain binds the adenine part of the FAD cofactor and is called the FAD-binding domain while the other, usually called the substrate domain, covers the isoalloxazine moiety of the cofactor and forms the major part of the active site around the isoalloxazine ring. A special feature of this flavoprotein family is the fact that a relatively large number of VAO members bind the FAD cofactor in a covalent manner. Among the wide range of carbohydrate oxidases, the subclass of polyol oxidases shows a low level of exploration, and at present only a few oxidases acting on polyols have been identified, narrowing biocatalytic exploitation of this class of oxidative enzymes. A VAO homologue belonging to this oxidase subclass (alditol oxidase, AldO) has been recently identified in the proteome of *Streptomyces coelicolor* A3(2) and biochemically characterized (*5*). The enzyme has been shown to be industrially relevant, as it can be used in a variety of applications. AldO is a soluble monomeric flavoprotein of 45.1 kDa, in which the flavin cofactor is covalently bound to the polypeptide chain through His46. Biochemical investigation has shown that AldO performs selective oxidation of only one of the terminal primary hydroxyl groups of alditols (Figure 1).

[†] The financial support by the Italian Ministry of Science (PRIN06 and FIRB programs), and the Petroleum Research Fund (46271-C4), administered by the American Chemical Society, is gratefully acknowledged.

[‡] Coordinates and structure factors have been deposited with the Protein Data Bank with the accession codes 2vfr, 2vfs, 2vft, 2vfu, and 2vfv.

* Author to whom correspondence should be addressed. (A.M.) Tel: +390382985534; fax: +390382528496; e-mail: mattevi@ipvgen.unipv.it. (M.W.F.) Tel: +310503634345; e-mail: m.w.fraaije@rug.nl.

[||] University of Pavia.

[§] University of Groningen.

[1] Abbreviations: VAO, vanillyl-alcohol oxidase; AldO, alditol oxidase; rmsd, root-mean-square deviation.

10.1021/bi701886t CCC: $40.75
Published on Web 12/23/2007

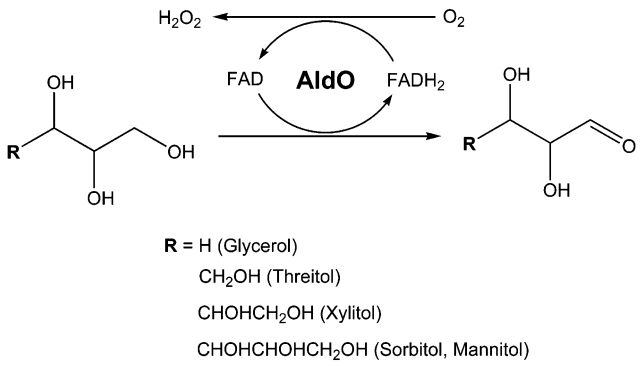

FIGURE 1: Reaction catalyzed by AldO.

While xylitol (five carbons) and sorbitol (six carbons) are the best substrates, L-threitol (four carbons) and D-mannitol (six carbons) are less good substrates, as can be seen from their relatively high K_m values (*5*). This illustrates that the enzyme is able to distinguish between structurally related polyols. The reaction catalyzed by AldO is a typical two-electron flavin-mediated oxidation of a terminal C−OH bond of a polyol substrate to the corresponding aldehyde, with the concomitant reduction of the flavin cofactor (Figure 1). The reduced flavin coenzyme reacts with oxygen to form hydrogen peroxide and the oxidized form of the flavin which completes the catalytic cycle.

Here, we report the structural characterization of AldO in the native oxidized state (1.1 Å resolution) and in complex with different polyol substrates (1.6−1.9 Å resolution). By means of high-resolution X-ray crystallography, we have unambiguously located the substrates into the enzymatic cavity. This provides insights into the mechanism of AldO-mediated regioselective oxidation reactions and its substrate specificity, explaining the reasons of the different enzymatic activity and selectivity in terms of molecular orientation, shape, and conformation of the catalytic cavity of the enzyme.

EXPERIMENTAL PROCEDURES

Protein Expression, Purification, and Crystallization. Native and Se-Met labeled recombinant alditol oxidase from *S. coelicolor* A3(2) were expressed and purified as described previously (*5*, *6*). The native protein was crystallized by the hanging-drop vapor diffusion method at 4 °C by mixing equal volumes of 14 mg/mL AldO solution in 50 mM KPi buffer pH 7.5 with reservoir solutions containing 0.1 M MES/HCl pH 6.5, 0.2 M $MgCl_2$ and 18−20% (w/v) PEG4000. Yellow crystals usually appear after 12 h and grow to optimal size (average dimensions 0.5 × 0.3 × 0.3 mm^3) in 3−4 days. Seleno-L-methionine-labeled crystals of AldO, grown as thin fragile plates (typical size 0.2 × 0.2 × 0.1 mm^3), were obtained in the same crystallization condition of wild-type protein after seeding the crystallization drop with microcrystals of native AldO. Without seeding, it was impossible to obtain crystals suitable for X-ray analysis. Substrate incorporation was achieved by soaking the wild-type AldO crystals in a solution consisting of 0.1 M MES/HCl pH 6.5, 0.2 M $MgCl_2$, 25% (w/v) PEG4000, 17.5% sucrose, and 25 mM substrate for 3 h. Monitoring the crystal color under a microscope during soaking experiments allowed an evaluation of the incorporation of substrate: because of the interaction of the covalently bound flavin of the enzyme with the polyol used for the soaking experiment, the crystal color gradually changed from intense to pale yellow. This indicates that the crystalline enzyme reacts with the substrate, resulting in the accumulation of the reduced form of the cofactor.

Data Collection, Structure Solution and Refinement. X-ray diffraction data were collected on a Rigaku R-Axis IV in-house rotating anode source and at the ID23-EH1 and ID14-EH3 beamlines of the European Synchrotron Radiation Facility in Grenoble, France (ESRF). Data processing and scaling were carried out using MOSFLM (*7*) and programs of the CCP4 suite (*8*). The detailed data collection statistics for the collected datasets are shown in Table 1. The structure of AldO was solved by SAD on the Se-edge using SHELXD (*9*) and SHARP (*10*) and seven out of eight Se atoms present in the asymmetric unit of the Se-Met AldO crystals were identified. After combination of the Se-SAD data at 2.4 Å resolution with native data at 1.1 Å, the initial SAD phases had a mean figure of merit of 0.55, and of 0.77 after density modification using SHARP and DM (*11*). The experimental

Table 1: X-ray Data Collection Statistics

data collection	native	Se-SAD	xylitol	sorbitol	mannitol	sulfite
space group	*C*2	*C*2	*C*2	*C*2	*C*2	*C*2
a (Å)	106.02	106.04	108.96	107.18	106.96	105.56
b (Å)	68.61	68.60	67.10	66.62	65.93	68.45
c (Å)	57.98	58.41	59.81	59.13	58.85	57.96
β (deg)	95.15	95.30	94.83	95.09	94.49	95.19
X-ray source	ESRF ID23-EH1	ESRF ID23-EH1	ESRF ID14-EH3	ESRF ID14-EH3	rotating anode	rotating anode
wavelength (Å)	0.873	0.979	0.931	0.931	1.542	1.542
resolution range (Å)	57.7−1.1	29.5−2.3	33.5−1.6	37.9−1.6	19.9−1.9	19.9−1.7
observations (*N*)	605075	245906	176172	264683	96830	132633
unique reflections	167187	18661	53338	54653	32193	43108
completeness[a] (%)	100.0 (100.0)	100.0 (100.0)	94.1 (85.1)	99.9 (100.0)	99.9 (100.0)	98.5 (97.1)
multiplicity[a]	3.6 (3.6)	13.2 (8.5)	3.3 (3.3)	4.8 (4.8)	3.0 (2.9)	3.1 (3.0)
anom completeness (%)[b]	−	99.4	−	−	−	−
anom multiplicity (%)[b]	−	6.7	−	−	−	−
R_{Cullis}[a,c]	−	0.715 (0.739)	−	−	−	−
anom phasing power[a,d]	−	1.295 (1.217)	−	−	−	−
R_{sym}[a,d]	0.119 (0.430)	0.126 (0.217)	0.054 (0.498)	0.054 (0.243)	0.098 (0.542)	0.036 (0.094)
I/σ_I	9.0 (3.0)	21.9 (12.0)	16.3 (1.7)	21.5 (5.2)	12.4 (1.9)	24.9 (10.9)

[a] Highest shell in parentheses. [b] Completeness calculations treat Friedel pairs as separate observations. [c] $R_{Cullis} = (\sum||F_{PH+}(obs) - F_{PH-}(obs)|-|F_{PH+}(calc) - F_{PH-}(calc)||)/\sum|F_{PH+}(obs) - F_{PH-}(obs)|$. [d] Anomalous phasing power $= (\sum|F_H i|)/(\sum||F_{PH+}(obs) - F_{PH-}(obs)|- |F_{PH+}(calc) - F_{PH-}(calc)||)$. [e] $R_{sym}=\sum_{\boldsymbol{h}}\sum_i |I(\boldsymbol{h})_i - \langle I(\boldsymbol{h})\rangle|/\sum\langle I(\boldsymbol{h})\rangle$, where $I(\boldsymbol{h})_i$ is the scaled observed intensity of the ith symmetry-related observation for reflection $\boldsymbol{h}$ and $\langle I(\boldsymbol{h})\rangle$ is the average intensity.

Table 2: Statistics for Least-Squares Refinement of AldO Structures

	native	xylitol	sorbitol	mannitol	sulfite
PDB file name identifier	2vfr	2vfs	2vft	2vfu	2vfv
resolution[a]	57.7−1.1	33.5−1.6	37.9−1.6	19.9−1.9	19.9−1.7
protein atoms (*N*)	3273	3104	3124	3103	3166
ligand atoms (*N*)	54	64	66	65	58
solvent atoms (*N*)	860	356	560	439	525
R_{cryst}[b,c]	0.139 (0.191)	0.175 (0.342)	0.152 (0.207)	0.153 (0.248)	0.152 (0.205)
R_{free}[b]	0.165 (0.208)	0.211 (0.398)	0.179 (0.278)	0.199 (0.307)	0.184 (0.259)
mean B-factors					
protein + FAD	7.32	18.25	14.09	16.28	8.75
water	23.81	31.86	30.23	31.41	18.25
ligand	6.81	20.93	23.66	13.19	9.68
rmsd bond lengths (Å)	0.015	0.018	0.019	0.019	0.015
rmsd bond angles (deg)	1.719	1.561	1.650	1.628	1.730

[a] All measured data have been included in the refinement. [b] Highest shell in parentheses. [c] $R_{cryst}=\sum |F_o - F_c|/\sum |F_o|$, where F_o is the observed structure factor amplitude, and F_c is the calculated structure factor amplitude.

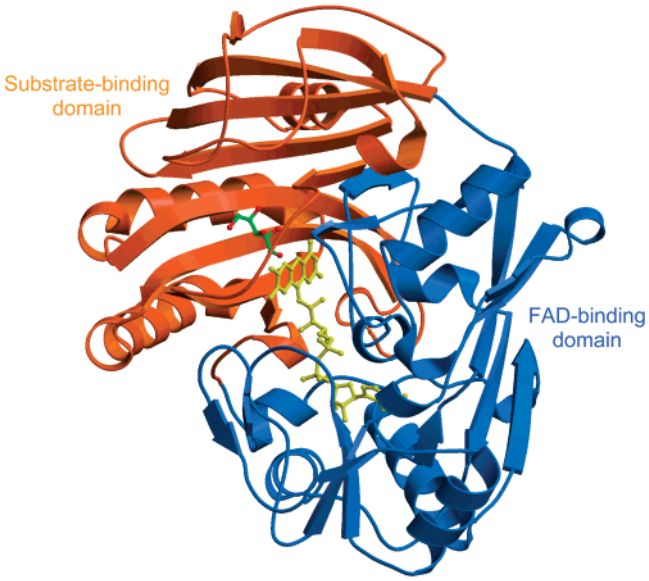

FIGURE 2: Overall crystal structure of alditol oxidase in complex with substrate xylitol. The ribbon diagram of the structure shows the two domains of AldO in blue and orange, respectively. The FAD cofactor is shown as yellow ball-and-stick. The substrate is shown as ball-and-stick, with carbon atoms colored in green and oxygens in red.

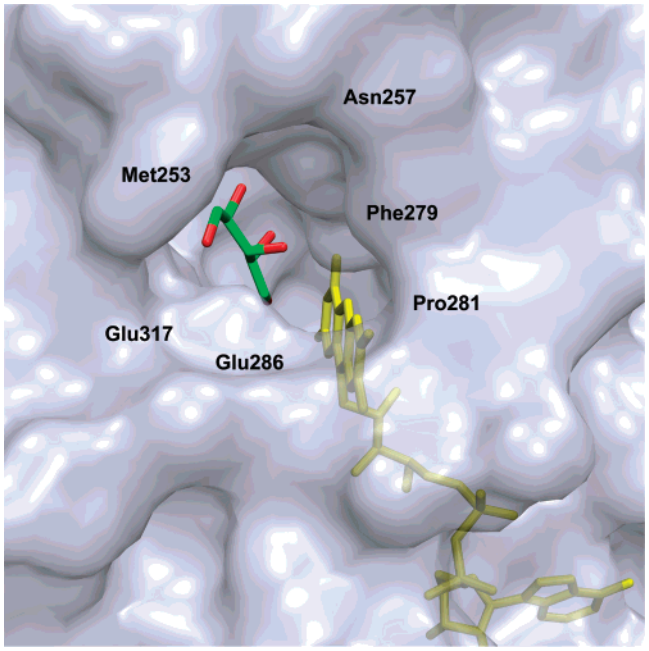

FIGURE 3: Close-up view of the AldO surface in proximity of the catalytic pocket. The xylitol substrate (carbons in green) is buried at the bottom of the binding site with the C^1-O^1H bond facing the C4a atom of the flavin ring (yellow). Residues that define the entrance of the catalytic pocket are labeled.

electron density map was of extremely good quality, and an almost complete initial model (405 amino acid residues out of 418) was automatically traced with ARP/wARP (*12*). Further manual model building and ligand docking were done with the graphics program COOT (*13*), and refinement was carried out with REFMAC5 (*14*). Refinement statistics are listed in Table 2. The final native AldO model contains one protein monomer per asymmetric unit, plus one FAD cofactor covalently bound to His46 and one Cl^- ion located on the surface. The stereochemistry of the final models was verified with PROCHECK (*15*) and COOT. Pictures were produced with PyMol (www.pymol.org), Molscript (*16*), and Raster3d (*17*).

RESULTS

Structure of Native Alditol Oxidase and Binding of the Flavin Cofactor. The crystal structure of recombinant native alditol oxidase (AldO) from *S. coelicolor* A3(2) has been solved by Se-SAD and refined to 1.1 Å resolution. AldO crystals are remarkably well ordered, resulting in electron density maps of outstanding quality. All refined structures (Table 2) exhibit good stereochemical parameters with no residue in the disallowed regions of the Ramachandran plot. AldO is a monomeric enzyme of 418 amino acid residues that contains one molecule of FAD cofactor per protein monomer, covalently attached to the protein as predicted by previous biochemical studies (*5*). The structure is composed of 15 α-helices and 18 β-strands, with the typical α+β fold shown in flavin-containing oxidases of the VAO family (*4*) and can be subdivided into two functionally distinct domains: an FAD-binding domain and a substrate-binding (cap) domain (Figure 2). A search of the Protein Data Bank with the program DALI (*18*) shows that the closest homologue of AldO is cholesterol oxidase from *B. sterolicum* (PDB entry 1I19) with a Z-score of 32.2, a root-mean-square deviation (rmsd) of 2.7 Å for 386 equiv Cα atoms and 19% sequence identity.

The FAD-binding domain comprises residues 1−180 and 380−418, whereas the substrate-binding domain consists of

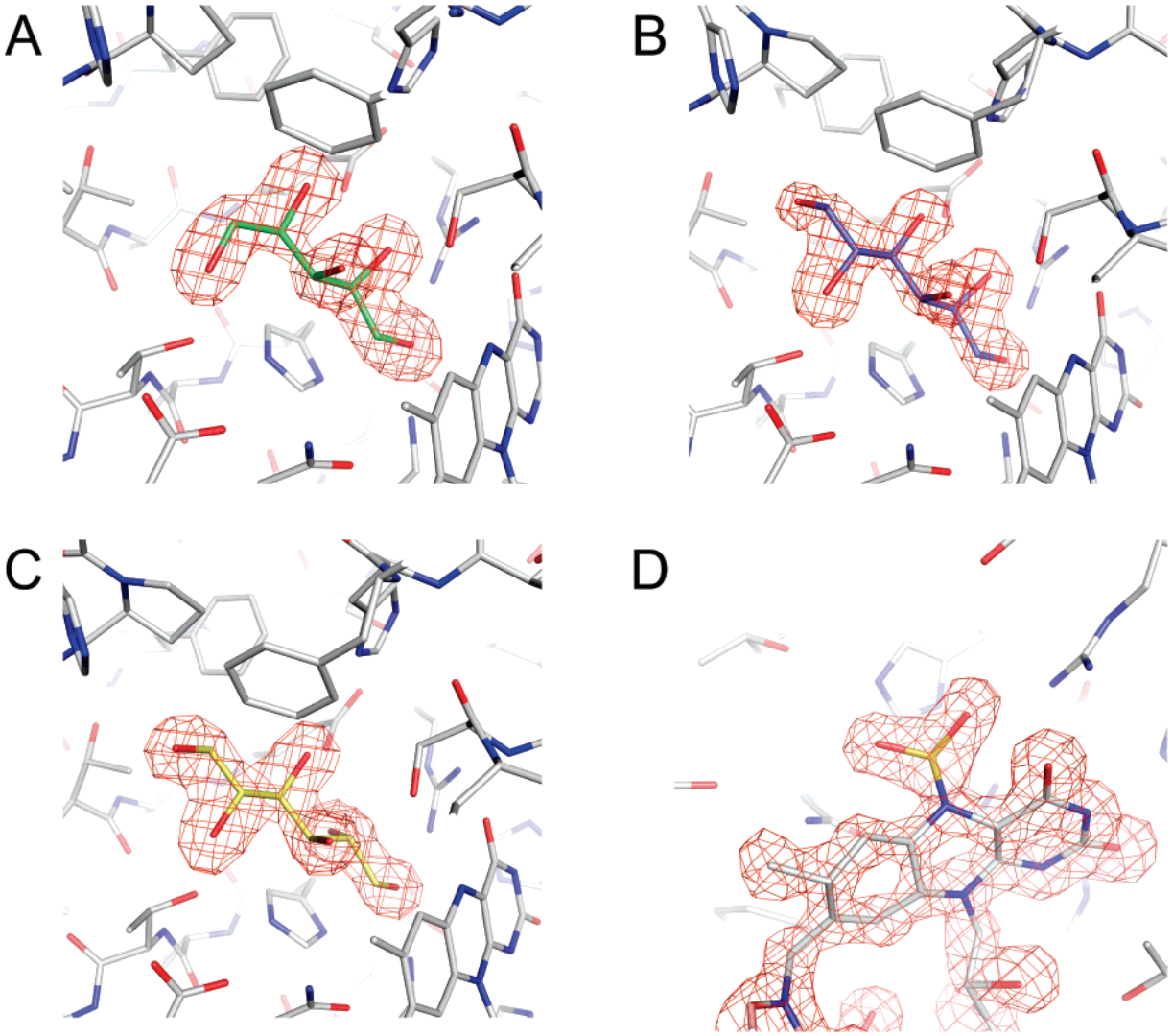

FIGURE 4: Electron densities from unbiased $F_o - F_c$ maps calculated at 1.6−1.9 Å resolution and contoured at 4.2 σ observed in the active sites of the complexes obtained by soaking native AldO crystals in xylitol (A), sorbitol (B), mannitol (C), and sodium sulfite (D). The maps were calculated prior inclusion of the ligand atoms in the refinement. In the cases of the soaking with substrates, the ligand electron densities have been interpreted as substrate molecules bound to the reduced enzyme. Protein carbon atoms are colored in gray, oxygens in red, nitrogens in blue, and sulfurs in yellow. Substrate carbon atoms are colored in green, blue, and yellow for xylitol, sorbitol, and mannitol, respectively.

residues 181−379. The cofactor is deeply buried in the protein structure and is involved in extensive contacts mainly with the FAD-binding domain. The pyrophosphate group of FAD is involved in several hydrogen-bonding contacts with main chain atoms of the loop described by residues ranging from Gly43 to Ser47. The cofactor is linked to the protein through a covalent bond between ND1 of the imidazole side chain of His46 and the C8-methyl group of the isoalloxazine ring. This histidine side chain approaches the isoalloxazine ring from the *re* face of the flavin. The high-resolution electron density maps clearly indicate that the flavin isoalloxazine ring adopts a planar conformation. It is located at the bottom of a narrow funnel-like cavity, which is occupied by several ordered water molecules. The cavity is connected to the protein external surface through an intricated network of amino acids, and its entrance is lined by Met253, Asn257, Phe279, Pro281, Glu286, and Glu317 (Figure 3).

Complexes of AldO with Polyol Substrates. The three-dimensional structures of the complexes of AldO with xylitol, sorbitol, and mannitol (Figure 4a, 4b, 4c, respectively) have been determined by difference Fourier methods and refined to 1.6−1.9 Å resolution (Table 1). The high-resolution maps calculated from an AldO crystals soaked with different substrates revealed strong electron density peaks in front of the *si* side of the flavin ring, located at the bottom of the cavity described in the previous section (Figure 3). When soaked with a polyol, the crystal color gradually changed from intense to pale yellow, indicating that the covalently bound flavin of AldO is reacting with the soaking compound and that the flavin is mostly reduced in the soaked crystals. Despite the high resolution of the diffraction data, it was impossible to unambiguously discriminate solely on the basis of the electron densities between the presence of a bound substrate (polyol) or product (aldose). High substrate concentrations (25 mM) were required in soaking experiments to obtain the enzyme−ligand complexes. This suggests that the crystalline enzyme initially is reduced by the substrate and, after dissociation of the aldose product, forms an abortive substrate-reduced enzyme complex (Figure 4). However, we cannot rule out that a mixture of products and substrates are actually bound to the crystalline enzyme molecules.

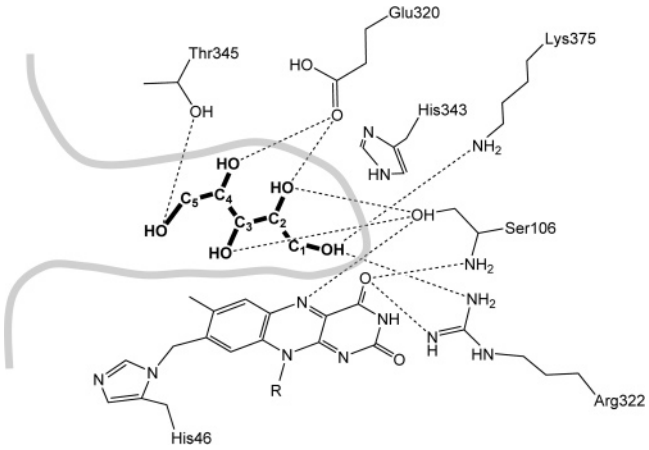

FIGURE 5: Schematic representation of the AldO substrate-binding site with reference to xylitol. Dashed lines represent hydrogen bonds. Solvent-accessible area is indicated as a light-gray line on the left of the image, showing that the substrate is docked at the bottom of the catalytic pocket.

We first consider the complex with xylitol, the best known substrate of AldO (*5*). Xylitol is positioned at the bottom of the active-site funnel through hydrogen-bonding interactions of its hydroxyl groups with Ser106 (atoms O^2 and O^3 of the substrate), Glu320 (O^2 and O^4), and Thr345 (O^5), respectively (Figures 5, 6a). In addition, the substrate O^1 atom establishes hydrogen bond interactions with two positively charged groups: the NZ atom of Lys375 and the guanidinium moiety of Arg322. The presence of residue His343, located as a back-door of the catalytic cavity, defines the size and shape of the substrate-accessible area in front of the flavin. As a result, the aliphatic chain of the substrate is "sandwiched" between the imidazole ring of the side chain of His343 and the flavin ring (Figure 6b). This arrangement places the C^1-O^1H bond of the polyol right in front of the C4a atom of the flavin ring, in an orientation for the oxidation event that can be typically identified for a hydride-transfer mechanism. The crucial role of His343 has been confirmed by site-directed mutagenesis: the His343Ala mutant is totally inactive (data not shown). The C^1-O^1H bond of the substrate is almost parallel to the flavin isoalloxazine ring, with a distance between the C^1 atom of the substrate and the N5 atom of the flavin of 3.4 Å, similar to that of VAO in complex with its substrates (*19*).

Xylitol binding does not cause any significant conformational change. The rmsd between the native and the xylitol-bound structure is 0.50 Å for all Cα atoms. Also, the active site is essentially indistinguishable from that of the native structure; remarkably, there is an exact superposition between the positions of the ordered waters in the ligand-free structure and the positions of the substrate OH groups. In this regard, the substrate can be considered as a plug located in the bottom of the funnel. On the basis of the changes of the crystal color (see above), the flavin in the soaked crystals is reduced. The electron density does not indicate any change in the conformation and stereochemistry of the cofactor upon reduction and ligand binding.

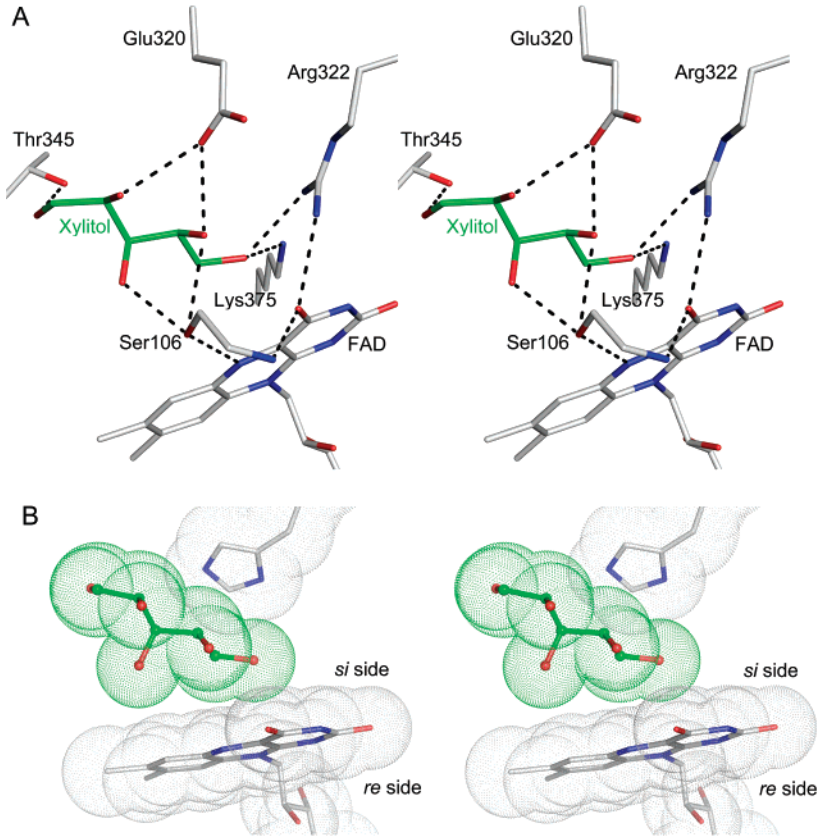

FIGURE 6: Three-dimensional structure of AldO active site with bound xylitol. (A) Stereoview of the amino acid arrangement around the substrate and the flavin cofactor when xylitol is bound in the catalytic pocket. Hydrogen bonds are shown as dashed lines. Atom colors are same as in Figure 4A. (B) Spacefill representation of the substrate docking into AldO catalytic cavity. The orientation of the imidazole ring of His343 constrains the substrate to place the C^1-O^1H bond right in front of the C4A atom of the flavin ring, in the proper orientation for the oxidation event that involves hydride transfer.

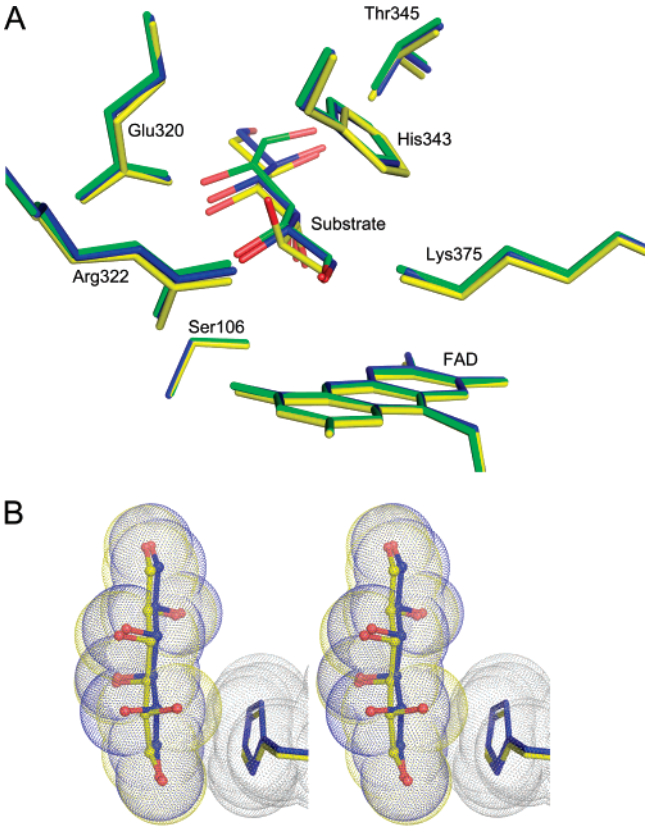

FIGURE 7: Structural comparison of the spatial arrangement in the different AldO−substrate structures. (A) Superposition of the three-dimensional structures of AldO in complex with xylitol (green), sorbitol (blue), and mannitol (yellow). Amino acids involved in direct interactions with the substrates are labeled. (B) Spacefill representation of the interaction between His343 and sorbitol and mannitol, respectively. Substrates are shown as ball-and-sticks with carbon atoms and van der Waals spheres colored as in Figure 7a and oxygen atoms in red. The spacefill representation highlights the difference between the mannitol and sorbitol complexes with respect to the steric hindrance of the C^2-O^2H bond in the direction of the imidazole ring of His343.

The superposition of the structures obtained by soaking AldO with different polyols (Figure 7a) indicates only very small differences in the arrangement of the amino acids located in the catalytic cavity. In particular, the arrangement of sorbitol (six-carbon skeleton) is strikingly similar to that of xylitol (five-carbon skeleton), with the $C^1-C^2-C^3-C^4$ atoms perfectly superimposed, showing the same network of interactions. The same interactions are highlighted also in the AldO-mannitol (six-carbon skeleton) complex, although the different chiral volumes of the C^2 atoms do not allow a perfect superposition. In this case, the substrate is forced to orient the C^2-O^2H in a direction that is opposite to that of the other two substrates (Figure 7b), creating a tight steric contact with the imidazole ring of His343. As this conformation is sterically unfavorable, it explains the 2 orders of magnitude lower catalytic efficiency for the oxidation of mannitol compared to the ones of xylitol and sorbitol (*5*).

Complex of AldO with Sodium Sulfite. Similar to several flavin-containing oxidases, AldO is capable of interacting with sodium sulfite generating an adduct on the N5-atom of the isoalloxazine ring of the FAD cofactor (*5*, *20*). By soaking native AldO crystals with a solution containing a high concentration of Na_2SO_3 it has been possible to obtain bleaching of the yellow color of the oxidized flavin in the protein crystals, because of the formation of the covalent adduct between FAD and sulfite. The analysis of the difference Fourier electron density maps showed a heavily distorted flavin ring (Figure 4d), with the sulfur atom located right in front of the N5 atom of the isoalloxazine ring on its *si* side.

DISCUSSION

Structural Interpretation of AldO Catalytic Mechanism. Docking of substrates into the AldO catalytic cavity shows a "lock and key" mechanism in which the pawls of the lock are represented by the side chains of Ser106 and Glu320. The five hydroxyl groups bound to C^1, C^2, C^3, C^4, and C^5 of the polyol substrates are all involved in a well-defined hydrogen-bonding network that explains at molecular level the preference of AldO for polyols rather than other aliphatic primary alcohols, diols, and carbohydrates (*5*). In addition, no side chains have been identified to interact with the C^6-OH group of polyols longer than xylitol. Together, all these features explain the worse catalytic efficiency of AldO (mainly related to higher K_m values) toward substrates shorter than xylitol (glycerol, and L-threitol) or longer (mannitol and sorbitol).

The presence of His343 forces the substrate to expose his C^1-O^1H bond with the C^1 pointing toward the flavin N5 atom with a distance of 3.4 Å, in a conformation that clearly promotes oxidation of this bond via a hydride transfer mechanism (*21*, *22*) (Figures 5, 6a). The superposition of AldO and its closest structurally similar homologue cholesterol oxidase (*23*) shows several differences in the surroundings of the flavin ring, although they share overall similarity in fold and mechanism of action. However, some residues identified as responsible for substrate activation and stabilization are conserved; in particular, Arg322 (Arg477) and Lys375 (Lys554) are located at the same position and in the same orientation in both enzymes. These residues may be involved in activating the substrate, creating a cluster of hydrogen bond donors that assist the deprotonation of O^1 atom of the polyol. In particular, the short H-bond distance of Lys375 (2.8 Å) and Arg322 (3.0 Å) with substrate O^1 atom strengthens this hypothesis. The major difference in the active site cavities of AldO and cholesterol oxidase is the lack of His343 in cholesterol oxidase (*23*, *24*). The absence of this sterically relevant residue makes the active site cavity of cholesterol oxidase large enough to accommodate the steroid substrate. It has been recognized that many bacteria contain an *AldO* gene orthologue (sequence identity ≥42%) (*5*). All the above-mentioned AldO active site residues are conserved in these orthologous proteins, indicating that they display an identical substrate acceptance profile.

The hydride transfer during polyol oxidation is coupled with the transformation of the tetrahedral terminal group of the polyol into the planar aldehyde of the corresponding linear aldose sugar. The sterical constrictions of the catalytic site do not allow the product to undertake the cyclization reaction inside the enzymatic cavity; thus, the released product of AldO catalyzed oxidation may be the linear aldose. In this view, cyclization is due only to the low stability of the linear aldose product and is not enzymatically assisted.

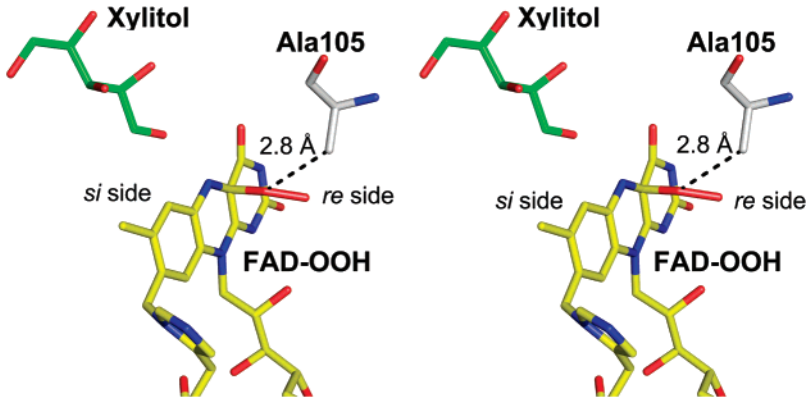

FIGURE 8: Model of an hydroperoxyflavin adduct on the *re*-side of AldO flavin cofactor. The picture shows the steric hindrance of the CH_3 moiety of Ala105 that might hamper formation of such an adduct.

Structural Explanation of AldO Stereoselectivity: Sorbitol versus Mannitol. The experimentally determined k_{cat} values for sorbitol and mannitol (six-carbon substrates that differ for the chirality at C^2) are 17 s^{-1} and 9.2 s^{-1}, respectively, while the K_m values are 1.4 mM and 36 mM, respectively (*5*). The difference in catalytic efficiency can be ascribed to a lower affinity for mannitol, more than to a slower catalytic process. The superposition of the three-dimensional structures of AldO in complex with these two epimers does not show any appreciable difference in the arrangement of the amino acids involved in the interactions with the substrates in the catalytic cavity (Figure 7a). Also the hydrogen-bonding network around the two substrates, although with different geometry due to the different chiral centers, is the same. However, the different orientation of the C^2-O^2H bonds in the two substrates provides an explanation of the different reactivity of AldO toward these substrates. While sorbitol does not show any difference in orientation of its polyol skeleton when compared to the most efficient substrate xylitol, the stereochemistry of mannitol forces the orientation of its O^2 atom in the direction of His343 (Figure 7b), in a stereochemically unfavorable conformation if compared to those of xylitol and sorbitol, with a distance between atom O^2 in mannitol and atom CD2 of His343 of only 3.0 Å. This explains the higher K_m value exhibited by this substrate.

Oxygen Reactivity. Biochemical characterization of AldO has classified this enzyme as a true flavin-containing oxidase, based on the reaction rates measured with molecular oxygen as electron-acceptor for flavin reoxidation (*5*). The high resolution of the solved structures of AldO in the native state and in complex with several substrates allowed us to make an analysis on the possible pathways that O_2 can undertake to reach the flavin ring during the catalytic cycle. A detailed kinetic analysis of AldO has shown that the enzyme operates via a ternary complex mechanism in which O_2 reacts with the enzyme−aldose complex. This requires molecular oxygen to reach the proximity of the flavin ring with product bound to the reduced enzyme. The analysis of the AldO catalytic cavity indicates that the *si* side of the FAD cofactor is obstructed by the presence of the substrate that plugs the bottom of the cavity itself (as shown in Figure 6b). This suggests that molecular oxygen is likely to approach the flavin from the *re* side, passing through a small tunnel identified by the presence of several highly ordered water molecules that may flow to the surface through a gate defined by residues Arg92, His95, His279, Glu270, and Ala277. Interestingly, the tunnel does not overlap with the suggested oxygen channel in cholesterol oxidase, as it is located in a totally different part of the protein structure (*23*, *24*). On the *re* side of the flavin, there is enough space to accommodate the oxygen molecule right in proximity of the isoalloxazine ring. However, the presence of the side chain of Ala105 seems to interfere with the formation of a hypothetical C4a hydroperoxyflavin intermediate (*25*, *26*) in the course of the oxidative half-reaction that generates hydrogen peroxide as a result of the two-electron transfer from $FADH_2$ to oxygen. A model of this intermediate built on the FAD cofactor of AldO (Figure 8) shows that this steric obstruction can be removed by a relatively small (1 Å) shift of the methyl group of Ala105. Therefore, the three-dimensional structure does not completely rule out occurrence of a hydroperoxyflavin intermediate, whose formation however has not been detected in stopped-flow studies (*5*).

Conclusions. AldO is an interesting enzyme from an industrial point-of-view because of the ease and high yield in protein production combined with the nonexclusive specificity and high reactivity toward different polyols. In this work we have elucidated structural details of this enzyme, explaining the reasons for substrate selectivity and thus putting down the bases for further developments in the usage of this protein for industrial purposes. The observation of the high-resolution three-dimensional structures of the enzyme−substrate complexes clearly identifies the hydride-transfer as the mechanism of catalysis in this oxidase. These data give a structural confirmation to biochemical data previously measured, unraveling the interactions between the amino acids, the flavin and the substrates that are responsible for the different reaction rates of AldO toward different polyol substrates. The investigation on the possible pathways adopted by molecular dioxygen in AldO, combined with the hypothesis of a ternary-complex mechanism for flavin reoxidation, allowed us to find a small cavity on the *re* side of the flavin that may host O_2 during the reoxidation step of the FAD cofactor. These high-resolution structural data will be useful for further studies in characterizing of the oxygen-mediated reoxidation of the flavin-containing oxidases.

REFERENCES

1. van Hellemond, E. W., Leferink, N. G., Heuts, D. P., Fraaije, M. W., and van Berkel, W. J. (2006) Occurrence and biocatalytic potential of carbohydrate oxidases, *Adv. Appl. Microbiol. 60*, 17−54.

2. Xu, F., Golightly, E. J., Fuglsang, C. C., Schneider, P., Duke, K. R., Lam, L., Christensen, S., Brown, K. M., Jorgensen, C. T., and Brown, S. H. (2001) A novel carbohydrate:acceptor oxidoreductase from *Microdochium nivale*, *Eur. J. Biochem. 268*, 1136−1142.
3. Ahmad, S. K., Brinch, D. S., Friis, E. P., and Pedersen, P. B. (2004) Toxicological studies on Lactose Oxidase from *Microdochium nivale* expressed in *Fusarium venenatum*, *Regul. Toxicol. Pharmacol. 39*, 256−270.
4. Fraaije, M. W., Van Berkel, W. J., Benen, J. A., Visser, J., and Mattevi, A. (1998) A novel oxidoreductase family sharing a conserved FAD-binding domain, *Trends Biochem. Sci. 23*, 206−207.
5. Heuts, D. P., van Hellemond, E. W., Janssen, D. B., and Fraaije, M. W. (2007) Discovery, Characterization, and Kinetic Analysis of an Alditol Oxidase from *Streptomyces coelicolor*, *J. Biol. Chem. 282*, 20283−20291.
6. Forneris, F., Rovida, S., Heuts, D. P., Fraaije, M. W., and Mattevi, A. (2006) Crystallization and preliminary X-ray analysis of an alditol oxidase from *Streptomyces coelicolor* A3(2), *Acta Crystallogr., Sect. F: Struct. Biol. Cryst. Commun. 62*, 1298−1300.
7. Leslie, A. G. W. (1999) Integration of macromolecular diffraction data, *Acta Crystallogr., Sect. D: Biol. Crystallogr. 55*, 1696−1702.
8. Collaborative Computational Project, Number 4. (1994) The CCP4 Suite: Programs for Protein Crystallography, *Acta Crystallogr., Sect. D: Biol. Crystallogr. 50*, 760−763.
9. Usón, I., and Sheldrick, G. M. (1999) Advances in direct methods for protein crystallography, *Curr. Opin. Struct. Biol. 9*, 643−648.
10. de La Fortelle, E., and Bricogne, G. (1997) Maximum-Likelihood Heavy-Atom Parameter Refinement for the Multiple Isomorphous Replacement and Multiwavelength Anomalous Diffraction Methods, *Methods Enzymol. 276*, 472−494.
11. Cowtan, K. (1994) dm: An automated procedure for phase improvement by density modification, *CCP4 ESF-EACBM Newsl. Protein Crystallogr. 31*, 34−38.
12. Perrakis, A., Morris, R. M., and Lamzin, V. S. (1999) Automated protein model building combined with iterative structure refinement, *Nature Struct. Biol. 6*, 458−463.
13. Emsley, P., and Cowtan, K. (2004) *Coot*: model-building tools for molecular graphics, *Acta Crystallogr. D60, 2126−2132.*
14. Murshudov, G. N., Vagin, A. A., and Dodson, E. J. (1997) Refinement of Macromolecular Structures by the Maximum-Likelihood Method, *Acta Crystallogr. D53*, 240−255.
15. Laskowski, R., MacArthur, M., Moss, D., and Thornton, J. (1993) PROCHECK: a program to check the stereochemical quality of protein structures. *J. Appl. Crystallogr. 26*, 91−97.
16. Kraulis, J. P. (1991) MOLSCRIPT: A Program to Produce Both Detailed and Schematic Plots of Protein Structures, *J. Appl. Crystallogr. 24*, 946−950.
17. Merritt, E. A., and Bacon, D. J. (1997) Raster3D: Photorealistic Molecular Graphics, *Methods Enzymol. 277*, 505−524.
18. Holm, L., and Sander, C (1996) Mapping the protein universe. *Science 273*, 595−602.
19. Mattevi, A., Fraaije, M. W., Mozzarelli, A., Olivi, L., Coda, A., and van Berkel, W. J. (1997) Crystal structures and inhibitor binding in the octameric flavoenzyme vanillyl-alcohol oxidase: the shape of the active-site cavity controls substrate specificity, *Structure 5*, 907−920.
20. Massey, V., Müller, F., Feldberg, R., Schuman, M., Sullivan, P. A., Howell, L. G., Mayhew, S. G., Matthews, R. G., and Foust, G. P. (1969) The reactivity of flavoproteins with sulfite. Possible relevance to the problem of oxygen reactivity, *J. Biol. Chem. 244*, 3999−4006.
21. Fraaije, M. W., and Mattevi, A. (2000) Flavoenzymes: diverse catalysts with recurrent features, *Trends Biochem. Sci. 25*, 126−132.
22. Fitzpatrick, P. F. (2004) Carbanion versus hydride transfer mechanisms in flavoprotein-catalyzed dehydrogenations, *Bioorg. Chem. 32*, 125−139.
23. Coulombe, R., Yue, K. Q., Ghisla, S., and Vrielink, A. (2001) Oxygen Access to the Active Site of Cholesterol Oxidase through a Narrow Channel Is Gated by an Arg-Glu Pair, *J. Biol. Chem. 276*, 30435−30441.
24. Sampson, N. S., and Vrielink, A. (2003) Cholesterol oxidases: a study of nature's approach to protein design, *Acc. Chem. Res. 36*, 713−722.
25. Mattevi, A. (2006) To be or not to be an oxidase: challenging the oxygen reactivity of flavoenzymes. *Trends Biochem. Sci. 31*, 276−283.
26. Massey, V. (1994) Activation of molecular oxygen by flavins and flavoproteins. *J. Biol. Chem. 269*, 22459−22462.

BI701886T